# Semi-automated shape analysis of dendrite spines from animal models of FragileX and Parkinson's Disease using Large Deformation Diffeomorphic Metric Mapping

G. Aldridge[1*], JT Ratnanather[2], ME Martone[3], M Terada[3], MF Beg[4], L Fong[2,3], E Ceyhan[2], AE Kolasny[2], T Brown[2], TN Tasky[2], EL Cochran[2], SJ Tang[2], DV Pisano[2], M Vaillant[2], MK Hurdal[5], JD Churchill[6], WT Greenough[1], MI Miller[2], MH Ellisman[3]

## Introduction

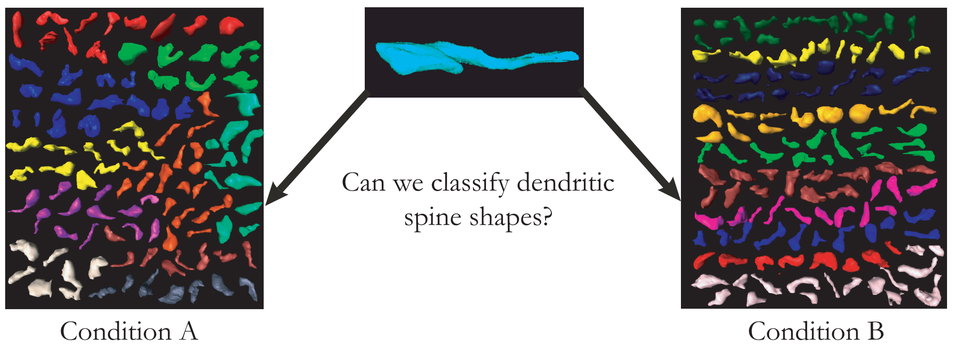


**Figure 1:** A fundamental question in neuroscience

• Several studies suggest that changes in dendritic spine structures cause physiological changes in, for example, the synaptic region that result in neurodegeneration and neurodevelopmental disorders [1]. Tissue from patients with Fragile-X syndrome (FXS) or Parkinson's Disease and mouse models of these disorders exhibit an increase in dendritic spine length and density. Thus the long term goal is to develop reliable and objective automated methods for classifying dendritic spine shapes as conceptualised in Figure 1.

• The discipline of Computational Anatomy (CA) provides the basis for the shape analysis [2]. CA synthesizes D'Arcy Wentworth Thompson's seminal ideas [3] in which transformations of local coordinate systems are used to compare anatomical structures.

• Briefly, CA is an anatomic model characterized by a quadruple $(\Omega,\mathcal{G},\mathcal{I},\mathcal{P})$ where $\Omega$ is the template coordinate space, $\mathcal{G}$ is a subset of diffeomorphisms on $\Omega$, $\mathcal{I}$ is the orbit (collection) of anatomical imagery under $\mathcal{P}$ which is the family of probability laws of anatomical variation on $\mathcal{I}$.

• Diffeomorphisms are smooth, invertible and differentiable maps that are modeled as evolution in time, or a flow $g_t$, $t\in[0,1]$ controlled by smooth velocity vector fields $v_t \in \mathcal{V}$, $t\in[0,1]$ (Figure 2). If $g_0 = g_0^{-1} = \mathrm{Id}$ is the identity map, the forward and inverse maps are given by

$$\frac{\partial g_t}{\partial t} = v_t(g_t) \quad \text{and} \quad \frac{\partial g_t^{-1}}{\partial t} = -(\nabla g_t^{-1})\, v_t$$

• Given two anatomical images $I_0, I_1 \in \mathcal{I}$ (Figure 2), the solution to the variational problem

$$\min_{v_t} \int_0^1 \|v_t\|_V^2 dt + \left\| I_1 - I_0(g_1^{-1}) \right\|^2$$

gives rise to the optimal changes of coordinates $\hat{g}_1$ such that $I_0(\hat{g}_1^{-1}) \approx I_1$ .

• The solution is determined from the Large-Deformation Diffeomorphic Metric Mapping (LDDMM) algorithm [4,5] which yields the arc length of the geodesic connecting the two images

$$d(I_0, I_1) = \inf \int_0^1 \|v_t\|_V dt$$

and thus the metric distance between the two images. Such metric distances provide a precise mathematical description of what shapes are similar and different.

• LDDMM has the ability to generate metric distances of anatomical structures at various scales from brain structures to sub-microscopic structures. LDDMM has been implemented and deployed on the Biomedical Informatics Research Network (BIRN; http://www.nbirn.net) and is currently being used in a morphometric study of the hippocampus in Alzheimer's Disease [6].

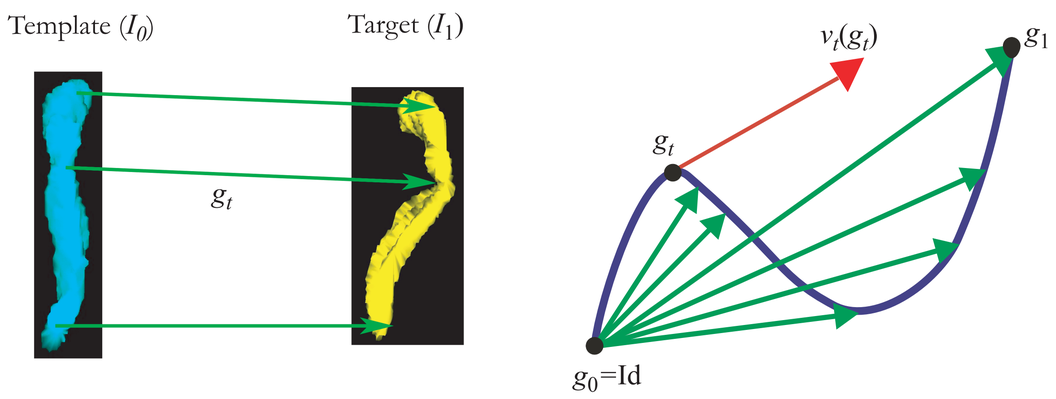


**Figure 2:** Generating diffeomorphisms between anatomical structures from a template spine to a target spine (left) with associated smooth velocity vectors (right).

**References**:

[1] Harris, K.M., Jensen, F.E., Tsao, B. (1992) Three-dimensional structure of dendritic spines and synapses in rat hippocampus (CA1) at postnatal day 15 and adult ages: implications for the maturation of synaptic physiology and long-term potentiation. J. Neurosci. 12, 2685-2705.
[2] Grenander, U., Miller, M.I. (1998) Computational Anatomy: an emerging discipline. Q. App. Math 56, 617-694
[3] Thompson, D.W. (1992) "On Growth and Form: The Complete Revised Edition", New York, Dover.
[4] Miller, M.I., Trouvé, A., Younes, L. (2002) On the metrics and Euler-Lagrange equations of Computational Anatomy. Ann. Rev. Biomed. Engng., 4, 375-405.
[5] Beg. M.F., Miller, M.I, Trouvé, A., Younes, L. (2005) Computing Large Deformation Metric Mappings via Geodesic Flows of Diffeomorphisms. Int. J. Comp. Vision, 61, 139-157.
[6] Jovicich, J., Beg, M. F., Pieper, S., Priebe, C., Miller, M., Buckner, R., Rosen, B. (2005) Biomedical Informatics Research Network: Integrating Multi-Site Neuroimaging Data Acquisition, Data Sharing and Brain Morphometric Processing. *In* 18th IEEE Symposium on Computer-Based Medical Systems (CBMS'05) (Eds: Tsymbal, A., Cunningham, P.), pp. 288-293.
[7] Martone, M.E., Zhang, S., Gupta, A., Qian, X., Price, D.L., Wong, M., Santini, S., Ellisman, M.H. (2003) The cell-centered database: a database for multiscale structural and protein localization data from light and electron microscopy. Neuroinformatics 1, 379-395.

[1]University of Illinois, Urbana IL
[2]Johns Hopkins University, Baltimore MD
[3]University of California, San Diego CA
[4]Simon Fraser University, Burnaby BC, Canada
[5]Florida State University, Tallahassee FL
[6]St Louis University, St Louis MO

**Center for Imaging Science http://cis.jhu.edu**

## Methods

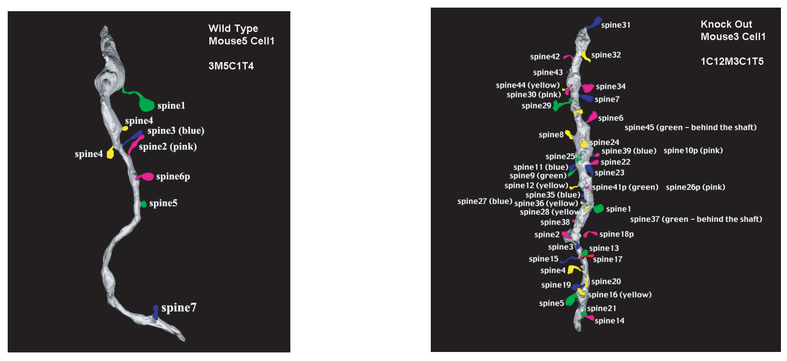


**Figure 3:** Reconstructed spines from wildtype (left) and knockout (right) mice from CCDB

• Pyramidial cells from layer V of primary visual cortex from FXS knockout (KO; n=2) and wildtype (WT; n=2) mice were injected with Lucifer yellow. Tissue was subsequently photooxidised and prepared for electron microscopy.

• Triangulated surface reconstructions of spiny dendrites were produced by manual contouring of tomographic reconstructions of neurons yielding 544 spines.

• The Cell-Centered DataBase (CCDB; https://ccdb.ucsd.edu/CCDB/index.shtml) [7] was used to upload and download original, segmented and reconstructed data for analysis (Figure 3).

• Reconstructed spines were checked for topological errors to ensure that triangulated surfaces were topologically equivalent to sphere via TopoCV (Topology Checker and Viewer; http://www.math.fsu.edu/~mhurdal/software/).

• 280 topologically correct spines were aligned with a standard coordinate system with respect to the smallest WT spine via similitude matching (scale or no-scale, rotation, translation) of 14 landmarks suitably placed on each spine. 2 landmarks were assigned to the neck and head and the remaining 12 obtained from groups of 4 evenly distributed landmarks at three equi-spaced sections between the head and the neck (Figure 4).

• LDDMM was applied to binarized images of the surfaces from which metric distances between the spines and the template (reference) spine were generated.

• LDDMM is computationally intensive requiring significant processing power and data storage especially in large-scale multi-site shape analysis [6]. In BIRN, LDDMM is utilized via supercomputing clusters such as the TeraGrid.

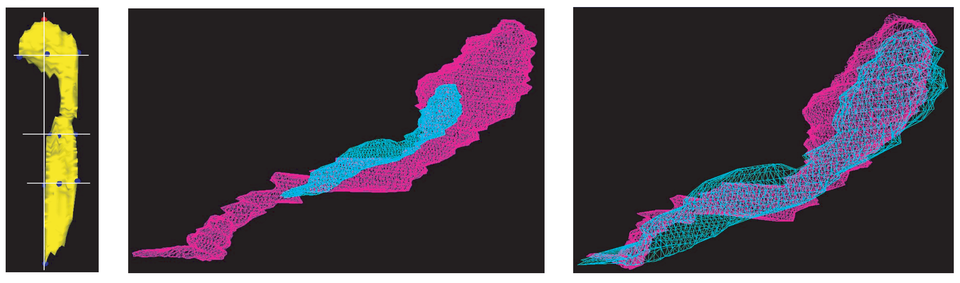

**Figure 4:** Similitude matching to align spines in a standard coordinate system with landmarks (left), no-scale (middle) and scale (right).

## Results

• Spine type was classified as one of double, filipodia, long mushroom, mushroom, stubby and thin [1] along with volume ($V$), surface area ($S$) and length between neck and head ($L$).

• Statistical analysis was performed on metric distances, condition (WT and KO) and spine type.

• For *unscaled* spines, there was significant difference between the two conditions ($p<<0.0001$, two-sample $t$-test). There was also significant difference across the six different types of spines ($p<<0.0001$, ANOVA). Metric distances correlated strongly with $V^{1/3}$ and $S^{1/2}$ ($R^2 = 0.9722$ and 0.9893 respectively) but weakly with $L$ ($R^2 = 0.6588$).

• For *scaled* spines, there was significant difference between the two conditions ($p<0.01$) and across the six different types ($p<0.075$).

• After accounting for $V$, $S$, $L$ and type of spine with ANOVA multiple test for multiple regression, there was significant difference in the condition of the scaled spines ($p<0.03$) but *not* for unscaled spines ($p=0.45$).


**Figure 5**: Deforming from target to template with the velocity vectors shown on the right.

## Discussion

• Metric distances can be used as a bio-marker to quantify dendritic spine shape in animal models of neurodegeneration and neurodevelopment.

• Analysis of dendritic spines from an animal model of Parkinson's Disease with blind knowledge of condition (Figure 1) and analysis of metric distances for each spine type are currently underway.

• Velocity vectors generated can be used to detect localized changes in the synapses (Figure 5).

**Research supported by:**

**NSF ACS-9619020, DMS-0101329, NIH P41-RR15241, P41-RR04050, P41-RR08605, R01-DA016602, P20-EB02013 and NSERC 31-611387**